On the decay of some odd isotopes of Pt, Au and Hg

by **A. de-Shalit***), **O. Huber**, and **H. Schneider**, Phys. Inst. der ETH., Zurich.

(4. XII. 51.)

———

Zusammenfassung: Der Zerfall der Kerne Pt[195]*, Au[195] und Au[199] wurde untersucht. Für die Messungen wurde eine Koinzidenzanordnung im β-Spektrometer benützt. Zerfallsschemen sowie Konversionskoeffizienten werden angegeben. Die Resultate werden diskutiert unter dem Aspekt des Schalenmodells und es wird nachgewiesen, dass alle angeregten Zustände in diesen drei Kernen, sowie auch im Hg[197], mit den Forderungen eines Einteilchenmodells nach MAYER verträglich sind.

Introduction.

The existence of a shell structure in nuclei has recently been determined in many different ways[1-3]. One usually notices that a certain property of nuclei, when plotted against the number of protons or neutrons in the nucleus, has a breakdown at certain "magic-numbers" which is interpreted as an indication for the beginning of a new shell.

Since the recognition of these magic-numbers, the first aim of a nuclear model has been to explain the closing of the shells at these numbers. This could be achieved by different models[4-8], and the further choice among them is dictated by the behaviour of each of them all along the shell.

The model of MAYER, which is usually considered to be the most successful one, is, at least for the ground states, a single particle model. The natural question is whether this single particle model can be extended to include also excited states, and to what an extent.

In order to calculate nuclear energy levels one may proceed in the following way:

An effective potential-well is postulated and the eigenstates in it are derived. One then considers the different configurations obtained

———

*) Now at the Palmer Phys. Lab. Princeton N. J., U. S. A.

by distributing those nucleons which are not in closed shells or sub-shells among the empty states. Each such configuration, which in the j-j-coupling scheme will be characterized by giving the occupation numbers n_i of the different sub-shells $(j_1^{n_1}, j_2^{n_2}, \ldots)$, has generally a number of terms arising from different relative orientations of the angular momenta of each nucleon.

In Mayer's model the lowest configurations are those in which there is exactly one odd occupation number (for odd A nuclei), and further, the lowest term in each configuration has the spin and parity of that state to which the odd particle belongs. That is: the lowest state of a configuration is a single-nucleon state.

A priori there are no serious objections to a situation in which the energy differences between the lowest terms of some different configurations will be smaller than the difference between the lowest term and the next one in the same configuration. That is: a single particle model could, in principle, exist for the first few excited states of odd nuclei. It could be realized, for instance, among particles moving in an oscillator potential-well slightly deformed. As is well known the energy levels of the (three dimensional) oscillator are degenerate with respect to the orbital angular momentum, and thus a slight deformation of this potential could give rise to a situation in which the "single particle levels" are lower than the excited terms of the lowest configuration.

As in Mayer's model the effective potential is a slightly deformed oscillator well, it might be well expected that the lowest excited states will in fact be single-particle ones.

This assumption is further strengthened by comparing the energy levels of odd-even nuclei with those of the neighbouring even-even ones. In general the first excited state of an even-even nucleus is higher than the first few levels in its odd-even neighbours. Even-even nuclei show a tendency of having more or less equi-distant levels of the same parity and whose spins differ by two units: $0 - 2 - 4$. This situation is characteristic for the terms formed by the excited states of a configuration of equivalent particles. Thus, if we really interpret these levels as such, the interpretation of the first excited states of odd-even nuclei as single particle ones would get further support. It should be noted that a big energy difference between the terms of a configuration of an even number of nucleons does not necessarily imply the same distance between the terms of a configuration of an odd number of nucleons. It serves merely to give an idea of the energy needed to "break" the pairing between the nucleons.

Another check on the validity of the single particle model for the first excited states of odd nuclei arises from the following simple considerations:

If the separation of the levels in a configuration is smaller than the separation between the lowest states of different configurations, one would expect to find similar decay schemes for two nuclei of which the one has n particles in the outmost shell and the other has n holes; the decay schemes of successive odd nuclei should be in principle different. If, however, the single particle model predominates, one should find, for odd A nuclei, exactly the same decay schemes all along the shell. That is:

> all odd A nuclei having their odd particle in the same sub-shell should have the same "set" of levels, the relative positions of which should vary continuously from one nucleus to the other[9]).

This work was undertaken in order to check if this result holds or not, and we chose for this purpose some odd A isotopes of Pt, Au, and Hg. The previous decay schemes of the isotopes we were about to examine would have definitely contradicted the above conclusion, as they were substantially different from each other. It therefore seemed worth while to check them with refined technique.

For this purpose we used a magnetic lens spectrometer supplemented by a coincidence arrangement which enables the measuring of the number of coincidences of each conversion line with all its "partners". This was technically done by placing a scintillation counter just behind the sample and taking coincidences between all the electrons measured in this scintillation counter and electrons of definite energy arriving at the Geiger counter on the other side of the spectrometer. This arrangement and its applications are described elsewhere[10,11]).

As for the samples, it was found most useful to prepare them by electrolysis. We could get very nice results by using as cathodes thin ($\sim 0{,}4$ mg/cm^2) gold foils which were floating on the solution to be electrolysed; we were thus sure that the active material was deposited on one side of the backing only, and the backing effects could be minimized.

In Chapter I we give experimental results on some odd N nuclei, and in Chapter II we shall discuss their decay schemes and others from the standpoint of Mayer's shell model.

*

<center>CHAPTER I.</center>

<center>**Spectroscopic measurements.**</center>

<center>**A. The Pt n-γ-products.**</center>

Spectroscopically pure Pt was irradiated by neutrons in the pile of HARWELL. Except for possible isotopes of short half-lives the periods found were of 18^h, $3,16^d$, $3,8^d$ and $\sim 70^d$.

The 18^h activity is known to be due to Pt^{197} decaying to the 77 keV and 268 keV levels in Au^{197} [12]). The $3,16^d$ activity is due to the β-decay of Au^{199} to Hg^{199} [13]); the Au^{199} is produced from the 29^m Pt^{199}. As will be shown later the $3,8^d$ activity arises from an isomeric transition in Pt^{195}. The 70^d activity, which was of a very low intensity, is probably due to some impurities of Ir which has a very high cross-section for the n-γ-reaction.

<center>§ 1. *Au^{199}; experimental results.*</center>

The electron spectrum of Au^{199} is shown in Fig. 1 together with the coincidence spectrum. The interpretation of these graphs is given in Table I.

<center>Table I.</center>

Energy of conv. line in keV	Interpretation	Relative intensity *)	Coincidence rate **)
1	M Auger		
7			
8,5	L Auger		
10,2			
36	50,6 L	5,83	12,2%
47	50,6 M	1,77	
50	K Auger		
74,6	157,5 K	22,7	8,6%
125,2	208,1 K	11,3	7,5%
145	157,5 L	33,7	8,1%
155	157,5 M	11,7	8,0%
194	208,1 L	2,0	7,1%
205	208,1 M	0,8	

*) These values were taken from another measurement with a better resolving power (1,5%).

**) Simple considerations show that the coincidence rate (number of coincidences per electron counted on the conversion line) at different points of the same line should be equal (indeed, deviations from this constancy were used to establish an overlaping of two different lines). The coincidence rates listed in the Table are averages of 4—5 points on each line; the fluctuations do not exceed 5% in any case and are less than 2% in most of them.
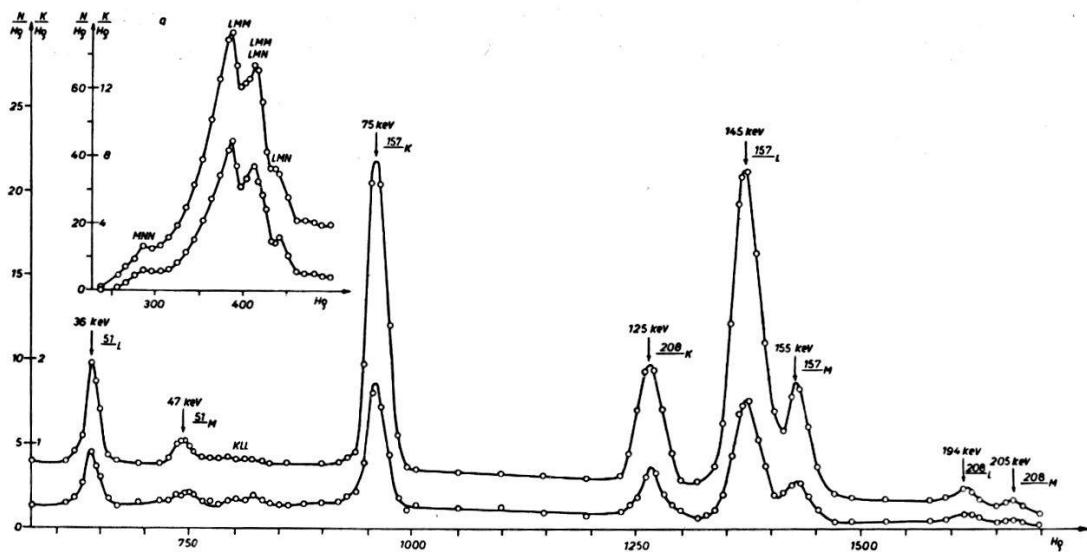
Fig. 1.

Electron spectrum of Au¹⁹⁹.

Upper curve – single counts;   lower curve – coincidences.

"a" was taken with an acceleration of 6 KeV.
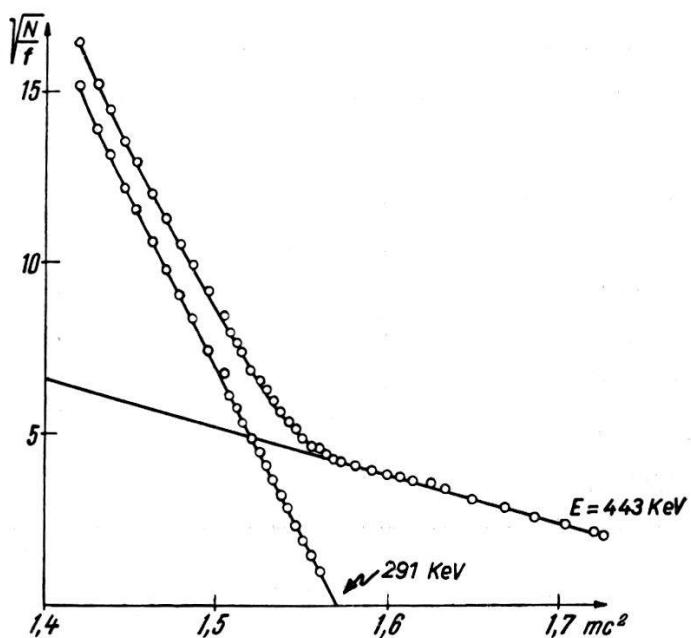
Fig. 2.

Kurie plot of β-spectrum of Au¹⁹⁹.

Fig. 2 shows a Kurie plot of the β-spectrum of Au^{199} which demonstrates the definite existence of two spectra of maximum energies 291 ± 5 keV and 443 ± 7 keV. Some 93% of the β-transi-
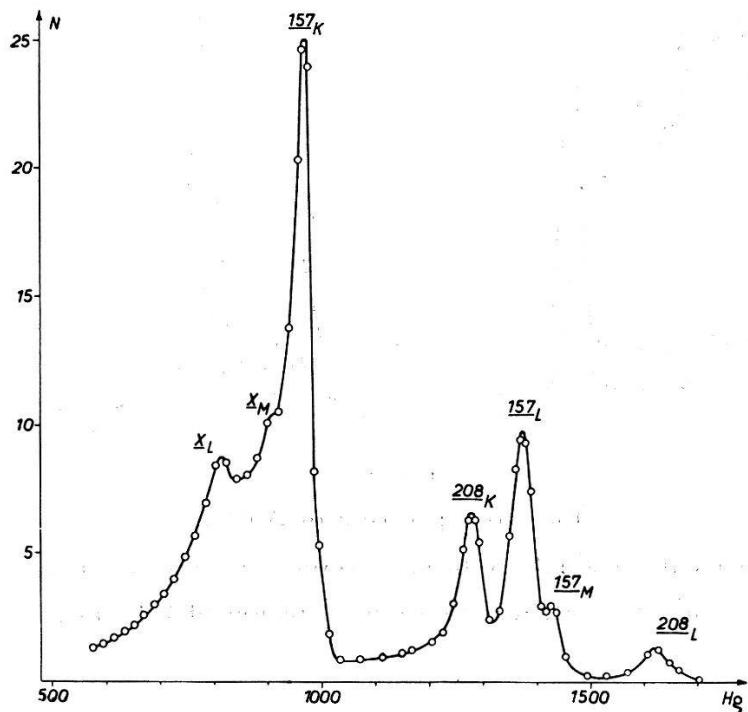
Fig. 3.

Photo-electrons of Au^{199}.

Table II.

Energy of photo line	Interpretation	Relative intensity
55 keV	X-rays L	
64 keV	X-rays M	
76 keV	157 K	25
127 keV	208 K	5,2
145 keV	157 L	9,5
155 keV	157 M	
196 keV	208 L	1,4

tions go to the excited states in Hg^{199}, whereas 7% decay directly to the ground state.

Fig. 3 shows the photo-electron spectrum of Au^{199} taken with an Au radiator of $2{,}6$ mg/cm^2 thickness. The interpretation of this graph is given in Table II.

An attempt to find angular correlation between the K conversion electrons of the 208 keV γ-ray and the rest of the spectrum, as well as between the K conversion electrons of the 157 keV γ-ray and the rest of the spectrum, gave negative results[14].

Discussion of experimental results; decay scheme.

From the $K - L$ differences it is seen that the 208 and the 157 keV γ-rays are most probably converted in Hg. The 51 keV γ-ray has an appreciable amount of coincidences so that this γ-ray, too, should be converted in the same nucleus, for otherwise it will have no partner to be in coincidence with.

These results agree with those of HILL[15]. No indication could be found for the lines of 24 keV, 70 keV, and 230 keV reported by BEACH et al.[13].

The difference in energy between the two main β-spectra (Fig. 2) indicates that they are leading to the initial and final levels of the 157 keV γ-transition. The fact that the 50,6 keV γ-ray and the 157 keV γ-ray sum up to give 208 keV, suggests that the first two are in cascade with each other and in parallel with the last one.

The absence of photo-electrons of the 51 keV γ-ray (Fig. 3) puts an upper limit of 10% for the ratio of the non-converted 51 keV γ-ray intensity to that of the X-rays. That is: if we denote by $\varkappa^{51}$ the total conversion coefficient of the 51 keV γ-ray ($\varkappa = N_e/N$, $\varkappa = \varkappa_K + \varkappa_L + \varkappa_M$), and if μ_{51} is the number of transitions via the 51 keV γ-ray per disintegration of Au^{199}, etc., we have:

$$\mu_{51} (1 - \varkappa^{51}) \leqslant 0,1 [\mu_{157} \varkappa_K^{157} + \mu_{208} \varkappa_K^{208}]. \tag{1}$$

It is clear that:

$$\mu_{51} \varkappa^{51} : \mu_{157} \varkappa_K^{157} : \mu_{208} \varkappa_K^{208} = Z^{51} : Z_K^{157} : Z_K^{208} \tag{2}$$

so that by introducing (2) into (1) one gets:

$$\left(\frac{1}{\varkappa^{51}} - 1\right) \leqslant 0,1 \frac{Z_K^{157} + Z_K^{208}}{Z^{51}}. \tag{3}$$

Inserting the values given in Table I for the relative intensities of the conversion lines one gets from (3):

$$\varkappa^{51} \geqslant 0,70. \tag{4}$$

To determine now whether the 51 keV γ-ray follows the 157 keV one or preceeds it, we note that in the first case the number of the 51 keV transitions is at least as big as that of the 157 keV ones, so that:

$$\frac{Z^{51}}{\varkappa^{51}} \geqslant \frac{Z^{157}}{\varkappa^{157}} \geqslant Z^{157}.$$

Therefore, assuming that the 51 keV γ-ray follows the 157 keV one, would lead to the relation

$$Z^{51} \geqslant 0{,}7\ Z^{157}$$

which is seen not to be the case (Table I). Thus, if they are at all in cascade, the 51 keV γ-ray preceeds the 157 keV one. This is also
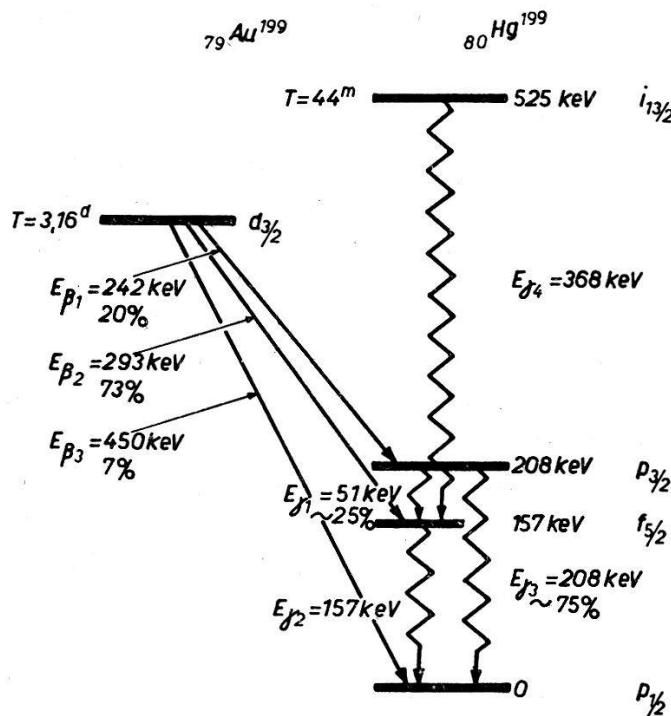
Fig. 4.

Decay scheme of Au^{199}.

confirmed by the decay of the 44^{m} isomeric state in Hg^{199}, since there is no indication of either a 51 keV or a 208 keV γ-ray, the only ones found being a 368 keV and the 157 keV γ-rays.

It is thus suggested that the decay scheme of Au^{199}-Hg^{199} is as shown in Fig. 4.

Our experimental data enable now a further check on this decay scheme, as well as the determination of the conversion coefficients and the different branching ratios.

We use the following symbols:

N = number of disintegrations per unit time,

Z = number of conversion electrons counted per unit time,

K = number of coincidences per unit time of a conversion line with all its partners,

ω_{Sc} = solid angle of the scintillation counter,

ω_{Sp} = solid angle of the spectrometer,

λ_i = branching ratios for the spectra,

μ = branching of the 208 keV level via the 51 keV transition,

$\varepsilon(p)$ = efficiency of scintillation counter for electrons of momentum p,

$f(p)$ = "shape" function of the spectrum $[\int f(p)\, dp = 1]$,

β = coincidence rate on a conversion line.

The following relations are easily proved:

$$
\left.
\begin{aligned}
Z^{51}_{L,M} &= N\,\lambda_1 \cdot \mu\,\omega_{Sp}\,\varkappa^{51}_{L,M} \\[1ex]
Z^{157}_{K,L,M} &= N\,(\lambda_2 + \lambda_1 \cdot \mu)\,\omega_{Sp}\,\varkappa^{157}_{K,L,M} \\[1ex]
Z^{208}_{K,L,M} &= N\,\lambda_1\,(1-\mu)\,\omega_{Sp}\,\varkappa^{208}_{K,L,M}
\end{aligned}
\right\} \tag{5}
$$

$$
\left.
\begin{aligned}
K^{51}_{L,M} &= Z^{51}_{L,M}\,\omega_{Sc}\left[\int f_1(p)\,\varepsilon(p)\,dp + \sum_{i=K,L,M}\varepsilon^{157}_i\,\varkappa^{157}_i\right] \\[1ex]
K^{157}_{K,L,M} &= Z^{157}_{K,L,M}\,\omega_{Sc}\left[\frac{\lambda_2}{\lambda_2 + \lambda_1\cdot\mu}\int f_2(p)\,\varepsilon(p)\,dp + \frac{\lambda_1\mu}{\lambda_2 + \lambda_1\cdot\mu}\times\right. \\[1ex]
&\qquad\left.\times\left(f_1(p)\,\varepsilon(p)\,dp + \sum_{i=L,M}\varepsilon^{51}_i\,\varkappa^{51}_i\right)\right] \\[1ex]
K^{208}_{K,L,M} &= Z^{208}_{K,L,M}\,\omega_{Sc}\int f_1(p)\,\varepsilon(p)\,dp
\end{aligned}
\right\} \tag{6}
$$

Combining (5) and (6) one gets:

$$
\beta_{51} - \beta_{208} = \omega_{Sc}\sum_{i=K,L,M}\varepsilon^{157}_i\,\varkappa^{157}_i = \omega_{Sc}\,\varkappa^{157}\sum\varepsilon^{157}_i\,\frac{Z^{157}_i}{Z^{157}}
$$

Hence:

$$
\varkappa^{157} = \frac{(\beta_{51} - \beta_{208})\,Z^{157}}{\omega_{Sc}\sum\varepsilon^{157}_i \cdot Z^{157}_i}. \tag{7}
$$

From the experimental values of β (Table I) we see that the coincidence rates for the K conversion lines are bigger than the ones for the corresponding L and M lines. This different coincidence rate for the K conversion lines is due to additional coincidences with the K Auger electrons. The efficiency of these electrons in the scintil-

lation counter arrangement is 50%[16]). Taking the Auger coefficient in Hg to be $0,06$[17]) one finds, with $\omega_{Sc} = 0,13$, that the Auger contribution to the coincidence rate for a K conversion line in Hg is $0,4\%$. This just explains the above difference. (That the difference in β is really due to coincidences with the K Auger electrons can be nicely shown by picking up from the crystal, with the help of an attenuator, only the big kicks caused by high energy electrons; in this case the K Auger electrons efficiency is very low in relation to the efficiency of the other electrons present[16]) and the coincidence rate is then exactly the same for all conversion lines of the same γ-ray.)

Subtracting the above $0,4\%$ from the coincidence rates on the K conversion lines given in Table I, we get the following average values for the coincidence rates on the three lines:

$$\beta_{51} = 12,2\% \qquad \beta_{157} = 8,1\% \qquad \beta_{208} = 7,1\% \qquad (8)$$

Substituting these values in (7) we get:

$$\varkappa^{157} = 0,50 \pm 0,02. \qquad (9)$$

To determine the conversion coefficient of the 208 keV γ-ray we use the photo-electron measurements. The efficiency of the Au radiator for 157 keV and 208 keV γ-rays was determined by interpolation from experimental calibrated points. The calibration was done with the 172 keV and 247 keV γ-rays of In^{111}. As is easily seen one has, for any decay scheme:

$$\frac{N_\gamma^{208}}{Z^{208}} : \frac{N_\gamma^{157}}{Z^{157}} = \frac{1 - \varkappa^{208}}{\varkappa^{208}} : \frac{1 - \varkappa^{157}}{\varkappa^{157}}$$

and we find experimentally

$$\frac{1 - \varkappa^{208}}{\varkappa^{208}} : \frac{1 - \varkappa^{157}}{\varkappa^{157}} = 0,83. \qquad (10)$$

Combining (9) and (10) we get:

$$\varkappa^{208} = 0,55 \pm 0,05. \qquad (11)$$

It should be noted that correcting factors which were neglected in evaluating (11), such as absorption of the γ's in the sample and its container, tend to increase this value. It is estimated that they could raise this value by 5—10%.

The relation (10), which is independant of the decay scheme, excludes the possibility that the 208 keV γ-ray will follow the 157 keV

one; for this value means that the conversion coefficients of both γ-rays are roughly equal, and thus if the 208 keV γ-ray would follow the 157 keV, its conversion electrons should be at least as numerous as those of the 157 keV γ-ray, and this is easily seen not to be the case (Table I).

Taking in addition into account the relatively high coincidence rate of the 51 keV γ-ray, which shows that it must be in coincidence with at least two lines or a line and a spectrum, one can see that only the given decay scheme is consistent with all the experimental data.

The small difference in the coincidence rate for the 157 keV γ-ray and for the 208 keV γ-ray is partially due to the 157 keV being in cascade with the 51 keV transition, and mainly to the fact that the spectrum leading to the 157 keV level is of a higher energy than the one leading to the 208 keV level, and thus has a bigger efficiency in the crystal. This was proved by noticing that this difference grew relatively bigger when only the higher kicks from the crystal were allowed to contribute to the measured coincidences.

By means of the conversion coefficients it is now easy to determine the branching ratios. We get:

$$0,22 \leqslant \mu \leqslant 0,30 \quad 0,20 < \lambda_1/(\lambda_1 + \lambda_2) \leqslant 0,23. \tag{12}$$

Table III.

The transitions in Hg[199].
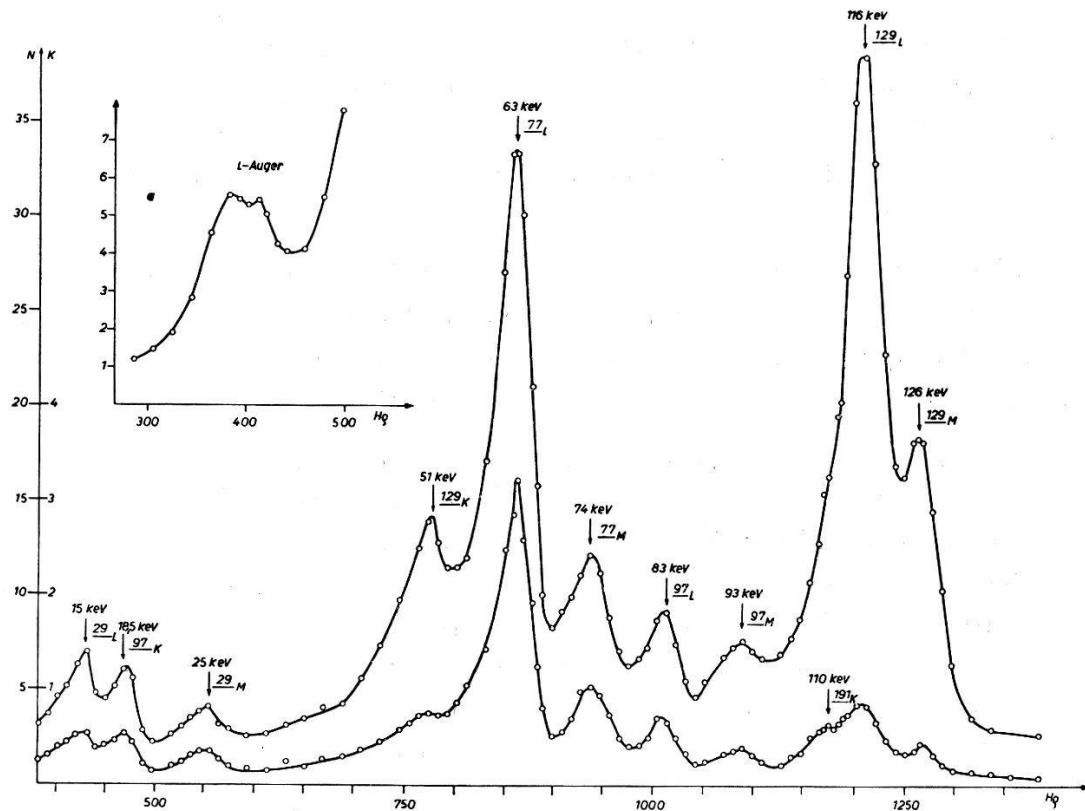
γ	$\varkappa\ (= N_e/N)$				$\alpha\ (= N_e/N_\gamma)$				K/L
	K	L	M	Tot	K	L	M	Tot	
51		$\geqslant 0,54$	$\geqslant 0,16$	$\geqslant 0,70$	—	$\geqslant 1,8$	$\geqslant 0,5$	$\geqslant 2,3$	—
157	0,17	0,25	0,08	0,50	0,33	0,50	0,17	1,0	0,67
208	0,44	0,08	0,03	0,55	0,98	0,17	0,07	1,22	5,65

§ 2. Pt^{195}; experimental results.

The Pt fraction of the neutron irradiated Pt decayed with two of the periods referred to above, namely: 18[h] and 3,8[d].

Fig. 5 shows the electron and the coincidence spectra of the Pt fraction. The interpretation of these measurements is given in Table IV.

The information one can get from these measurements is mainly qualitative rather than quantitative due to the fact that some of

Fig. 5. Electron spectrum of Pt^{195}.
Upper curve – single counts; lower curve – coincidences
"a" was taken with an acceleration of 6 KeV.

Table IV.

Energy of conv. line keV	Half life	Conv. in	Inter-pretation	Relat. int.*)	Coinc. rate **)
6,5	3,8^d	Pt	L Auger		
8,5	3,8^d	Pt			
15	3,8^d	Pt	29 L		14 %
18,5	3,8^d	Pt	97 K		11,5%
25	3,8^d	Pt	29 $M+N$		14,4%
51	3,8^d	Pt	129 K	1,0	7,3%
63	18^h	Au	77 L		
74	18^h	Au	77 M		
83	3,8^d	Pt	97 L	0,75	12 %
93	3,8^d	Pt	97 M	0,2	
110	18^h	Au	191 K		
116	3,8^d	Pt	129 L	3,8	3,2%
126	3,8^d	Pt	129 M	1,8	3,0%

*) The relative intensities were measured after the short period (18 h) had decayed; those not given could not be evaluated because of the absorption in the sample.

**) The coincidence rate measurements in the spectrometer were carried out after the 18 h activity had decayed, both in the neutron irradiated Pt and in a deuteron-irradiated Pt, which was also found to contain the 3,8 d activity in its Pt fraction.

the important lines are of such a low energy that the absorption of the electrons in the rather thick sample prevents any evaluation of their intensity. We therefore measured in addition the photo-electrons emitted from a 2,6 mg/cm² Au radiator. These are shown in Fig. 6.

Discussion of experimental results; decay scheme.

Our sample was not carrier-free and indeed absorbed considerably the low conversion lines. Nevertheless it is believed that the measured $K - L$ differences do represent their real values. The L Auger-electron group, which retains its form in our sample, supports this assumption. We thus conclude that the 97 keV and the 129 keV γ-rays are converted in Pt or Au; Ir is excluded. We can further
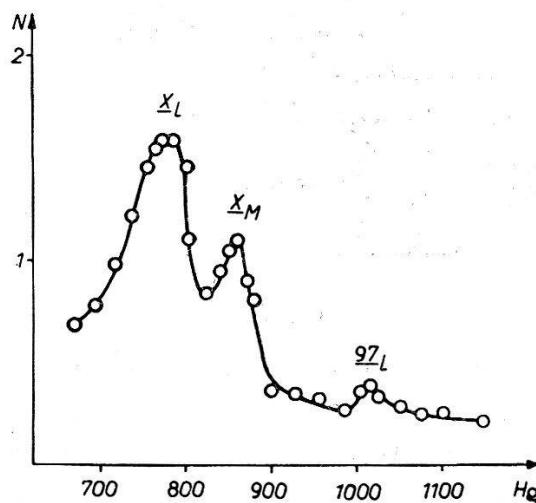
Fig. 6.

Photo-electrons of Pt[195].

exclude their conversion in Au from the absence of a β-spectrum. Thus an isomeric state in Pt is established.

The fact that all three lines: 29 keV, 97 keV, and 129 keV, have the same half-life suggests that they might be in cascade, if they all belong to the same nucleus.

The 129 keV and the 97 keV γ-rays are both converted in Pt; as the 29 keV γ-ray has coincidences and as the only electrons of the same period of 3,8^d are the conversion electrons of the 129 keV and 97 keV γ-rays, we conclude that the 29 keV γ-ray is also converted in Pt. For reasons to be given later we fix the order of the three γ-rays as shown in Fig. 7.

From the coincidence rate on the 97 keV conversion lines one concludes immediately that the 129 keV γ-ray is totally converted. (The 29 keV γ-ray contributes next to nothing to this coincidence rate because of the very low efficiency of the scintillation counter for its conversion electrons.)

The relative intensity of the 97 keV conversion electrons, compared to this of the 129 keV lines, could serve only as a rough lower limit to its conversion coefficient because of the uncertainties in the
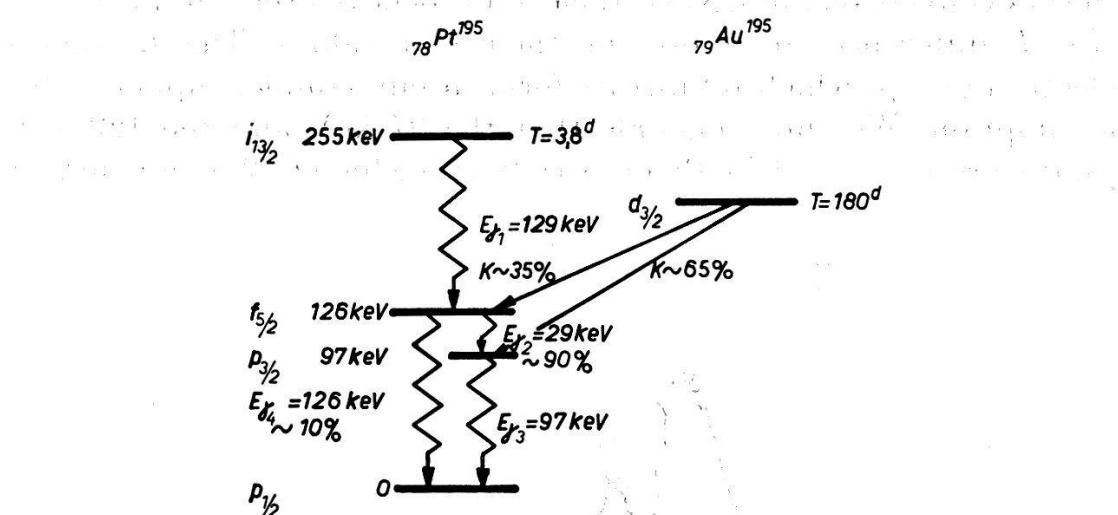
Fig. 7.

Decay scheme of $Au^{195} - Pt^{195}$.

absorption in the sample. We can therefore get a better value from the intensity of its photo-electrons as compared to the intensity of the X-rays photo-electrons (Fig. 6). For this we only need the relative efficiency of our radiator for L photo-electrons of the Pt X-rays and the 97 keV γ-ray. The L photo-electrons efficiency for Hg X-rays, 157 keV and 208 keV γ-rays could be easily determined from the photo-electron measurements in Au^{199} (Fig. 3), and from this we determined, by interpolation, our data. The resulting value for $\varkappa^{97}$ is:

$$\varkappa^{97} = 0{,}90 \pm 0{,}05. \tag{13}$$

To determine the true K/L ratio of the 97 keV conversion electrons we proceed in the following way: assuming $\varkappa^{129} = 1$ we see from Table IV that $\varkappa_L^{97} = 0{,}12$; combined with equation (13), we get:

$$(K/L)_{97} = 5{,}7. \tag{14}$$

Concerning the 29 keV γ-ray one can say that $\varkappa_L^{29} \geqslant \varkappa_K^{97}$, since the absorption of the 29 L line is bigger than that of the 97 K, and the experimental peaks are roughly equal (Fig. 5). Thus:

$$\varkappa_L^{29} \geqslant 0,75. \tag{15}$$

It is difficult to draw any quantitative results from the measurements of the coincidence rates for each of the lines. Most of the conversion lines with which we have to do in this case are of such a low energy that they fall on the steep part of the efficiency curve of the crystal. Thus relatively small variations in the energy due to scattering of the electrons in the sample and in the backing affect strongly the efficiency, which cannot therefore be controlled.

The most outstanding feature of these coincidence measurements is the big difference in β between the K conversion line of the 129 keV γ-ray and its L and M conversion lines. This was checked in a number of samples, and always gave the same result. A satisfactory explanation for it, which will be much supported later, is the existence of another γ-ray, of energy nearly equal to 129 keV, with a higher coincidence rate and bigger K/L ratio than those of the 129 keV γ-ray. One notices immediately that the cross-over transition $29 + 97$ could fulfill these requirements if it were of low enough intensity to "hide" itself in the tails of the 129 keV conversion lines, and if it had a big enough K/L ratio. Its high coincidence rate will be explained by its being in cascade with the 129 keV γ-ray.

As the number of transitions via a 126 keV γ-ray (the cross-over transitions) is at any rate small, the 129 keV γ-ray is effectively in coincidence only with the 97 keV γ-ray in our coincidence arrangement (since the 29 keV conversion lines have zero efficiency at the crystal). Similarly the 97 keV γ-ray is effectively in coincidence only with the 129 keV γ-ray, whereas the 29 keV γ-ray is effectively in coincidence with both the 97 keV and the 129 keV γ-rays. Thus we should have:

$$\beta_{29} \sim \beta_{97} + \beta_{129}. \tag{16}$$

Inspection of Table IV shows that this is very nicely fulfilled if we take for β_{129} the value measured on the 129 L or 129 M lines, giving one further support to our decay scheme.

B. The Pt d-x.n products.

Pt was irradiated with deuterons in the cyclotron of the Instituut voor Kernphysisch Onderzoek in Amsterdam *). The Au fraction was separated electrolytically; it showed the known half-lives of: 39ʰ (Au 194), 180ᵈ (Au 195), 5,6ᵈ (Au 196), and 3,2ᵈ (Au 199)[13]. In the Pt fraction the 3,8ᵈ activity was found, and its spectrum agreed in all details with the 3,8ᵈ activity from the neutron-irradiated Pt. No activity of intensity comparable to the 3,8ᵈ one and with a longer half life was found in the Pt fraction.

§ 3. Au^{195}; experimental results.

The electron spectrum of the long lived Au^{195} is shown in Fig. 8, along with its coincidence spectrum. Although the decay of each line was not followed long enough to find small differences in their half-lives, it is believed they all have the same period since their ratios did not show any systematic increase or decrease. The interpretation of the spectrum is given in Table V together with the coincidence rate on some of the lines.

Table V.

Energy of conv. line in keV	Interpretation	Relat. inten.	Coinc. rate
8 10 12 }	L Auger		3,0%
15	29 L	9,0	2,9%
18,5	97 K	29,2	1,0%
24	29 M	3,1	2,5%
26,5	29 N	0,9	2,4%
49	126 K + KLL Auger		
51 59 62 }	K Auger		
83	97 L	9,2	0,6%
93	97 M + N	2,4	0,4%
113	126 L	0,55	0,4%
124	126 M	0,2	

*) We are deeply indebted to Prof. BAKKER for carrying out this irradiation in his institute.

The interpretation of the Auger lines as such is based on energy considerations as well as on the fact that they were the only ones to follow a "compound" half-life composed of all the initial half-lives present in the Au fraction.

Discussion of experimental results; decay scheme.

The most striking feature of these measurements is the reappearence of the 29 keV and 97 keV γ-rays previously found in the neutron-irradiated Pt. Unfortunately the Pt sample was much thicker than this carrier free Au sample, so that no comparison of the K/L ratios can be done. However, the facts that the $(L/M)_{97}$ ratio is the same in both cases and that the γ-rays agree so well in energy favour very much their being the same lines.
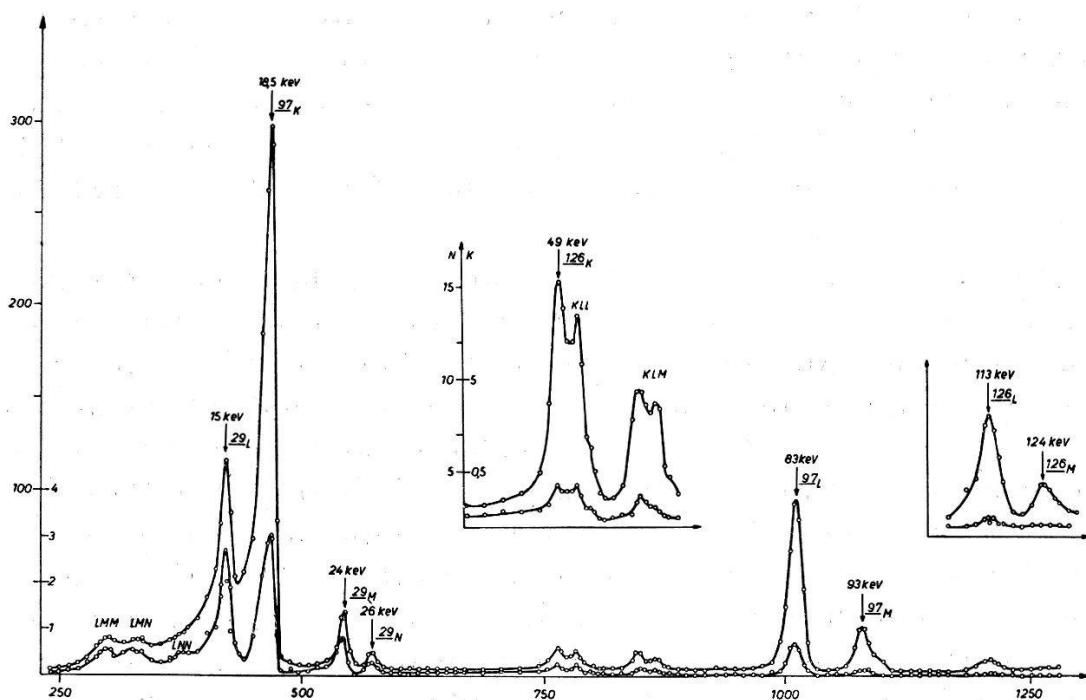
Fig. 8.

Electron spectrum of Au[195].

Upper curve – single counts; lower curve – coincidences.

Thus we justify, à posteriori, the assignment of mass number 195 to the 3,8^d isomeric state in Pt.

We further notice that although the Au sample is thinner than the Pt one, the 29 keV γ-ray is more intense in the second one. As the lines in the Au sample are formed through a K capture, this is only possible if the 29 keV γ-ray is above the 97 keV one.

A γ-ray of 126 keV and low intensity is seen to exist in the Au sample (Fig. 8). It was of great importance to clarify whether this

is the same one as the 129 keV γ-ray found in the Pt sample or not. If it were the same, then from intensity considerations one would conclude that the 129 keV γ-ray is above the others, and is thus responsible for the existence of the isomeric state in Pt. This would mean that the 129 keV γ-ray probably starts from a level of a high spin. As it is very improbable that a single level in Au will decay by K-capture to three levels in Pt which differ much in their spins, the identity of the "126" keV γ-ray and that of the 129 keV would imply the existence of an isomeric state in Au^{195} which decays to the isomeric state in Pt^{195} with roughly the same half-life of 180$^{\text{d}}$.

To clear this point it was not enough to measure the energies of the conversion lines, because the K conversion line of the 126 keV γ-ray overlaps partially the KLL Auger lines and the exact position of the maximum is not to be determined with the resolving power at our disposal. For the same reason it is impossible to draw any conclusions from the K/L ratio. The position of the L conversion lines will not settle the problem either, as variations in the relative intensity of the L_I, L_{II}, and L_{III} conversions may account for the coincidence of the "L" conversion lines of two slightly different γ-rays.

However, if the two lines are the same then the coincidence rates on both of them should be equal as can be seen by very simple considerations. Anyhow, any deviations from equality, caused by absorption in the sample and other by-effects, could only be in such a direction as to reduce the coincidence rate in our Pt sample. Comparison of Tables IV and V proves definitely that these two lines are different. The most natural assumption will now be that the 126 keV γ-ray is the cross-over transition (29 + 97), which is thus fed from the same level in Au as are the 29 keV and 97 keV γ-rays, and whose existence is also needed to explain the different coincidence rates on the 129 K and 129 L lines in the Pt sample. The decay scheme of Au^{195} would thus be as shown in Fig. 7.

A further check on this decay scheme is provided by considering the coincidence rates on the different lines; one should only remember in this connection that every line which is in coincidence with K Auger electrons (as is the case for all K conversion lines and for every conversion line which follows a K-capture) has, in Pt, a coincidence rate of 0,4% (see the discussion following Formula 7). We then see that the coincidence rates on the 126 keV conversion lines, as well as on those of the 97 keV γ-ray can be attributed to this effect. (The 97 K line is twice in coincidence with K Auger electrons: with those arising from the K-capture and with those

resulting from the filling of the holes in the K shell produced by the K conversion.) The additional coincidence rate on the 29 keV conversion lines arises from coincidences with the 97 keV conversion electrons; this rate fits with the coincidence rate on the 129 keV conversion lines in the 3,8^d Pt[195], which are also in coincidence with the same 97 keV γ-ray.

Using previously determined absorption curves of the counter foils we used[12]), and neglecting the absorption in the carrier free Au sample, we get, using the data of Table V:

$$(K/L)_{97} = 5,8 \pm 0,3 \quad (L/M)_{29} = 4,6 \pm 0,4 \tag{17}$$

in good agreement with (14) obtained in the Pt sample.

Using the values $\varkappa^{97} = 0,9$, $\varkappa_L^{29} = 0,76$ we get that 35% of the K-captures go to the 126 keV level and 65% go to the 97 keV level.

The total conversion coefficient of the 126 keV γ-ray could not be determined, but if one takes α_K from the tables of Rose et al.[18]), together with the K/L ratios from the experimental graphs for this ratio[19]), one finds that its conversion is not less than about 70% (for $E\,2$; $E\,1$ is very improbable), and thus that no more than 10% of the decays from the 126 keV level in Pt[195] are going via the cross-over transition.

Table VI summarizes the results obtained for the different γ-rays appearing in the decay of Au[195]-Pt[195].

Table VI.

γ	$\varkappa$				α				K/L
	K	L	M	Tot	K	L	M	Tot	
29		$\geqslant$0,75	$\geqslant$0,13	$\geqslant$0,88		$\geqslant$6,0	$\geqslant$1,3	$\geqslant$7,3	
97	0,74	0,13	0,03	0,90	7,4	1,3	0,3	9,0	5,8
126									<1,8
129	0,15	0,58	0,27	1	very big				0,26

*

CHAPTER II

Spin assignments.

§ 1. *Theoretical predictions.*

We shall now try to assign the spins and parities to the different states of the nuclei considered in the previous chapter as well as of other ones, and see to what extent can the shell-model be applied to these states and whether the rule referred to at the introduction holds or not. That is: we shall try to see whether successive odd nuclei which have their odd particle in the same sub-shell have or have not similar decay-schemes.

Let $E(j)$ be the energy of one nucleon in the state j, and let $E^*(j)$ be the energy of a pair of equivalent nucleons in the state j. That is:

$$E^*(j) = 2 E(j) - P(j) \tag{1}$$

where $P(j)$ is the pairing energy in the state j.

For the sake of simplicity we shall talk of the "multiplet" of all the terms arising from a certain configuration of nucleons coupled according to the j-j coupling scheme. This should not be confused with the spin multiplets in the L-S coupling scheme. The "ground state" of a certain configuration would be the lowest term in its multiplet. We shall measure all energies from the bottom of the potential well, so that all energies are positive, and a bigger energy means a less bound state.

Let us consider two states — j_1 and j_2 — of which the first is the lower; that is:

$$E(j_1) < E(j_2). \tag{2}$$

Let us further assume that j_1 is also a lower state for pairs of nucleons, i. e.:

$$E^*(j_1) < E^*(j_2). \tag{3}$$

In spite of these relations it is sometimes possible that the ground state of the configuration $j_1^{n-1} j_2^2$ will be lower than any other configuration of $n+1$ nucleons, especially the configuration $j_1^n j_2^1$, if n is the number of particles in the closed shell j_1 ($n = 2 j_1 + 1$).

To see what are the conditions for such a situation to be realized we note that the energy of the configuration $j_1^{n-1} j_2^2$ is:

$$E(n-1,2) = (n-2)/2\, E^*(j_1) + E(j_1) + E^*(j_2), \qquad (4)$$

and similarly:

$$E(n, 1) = (n/2)\, E^*(j_1) + E(j_2) \qquad (5)$$

so that:

$$E(n-1,2) - E(n, 1) = [E^*(j_2) - E^*(j_1)] - [E(j_2) - E(j_1)]. \qquad (6)$$

Therefore: the ground state of the configuration $j_1^{n-1} j_2^2$ will be lower than the ground state of any other configuration provided the following inequality holds:

$$[E^*(j_2) - E^*(j_1)] < [E(j_2) - E(j_1)] \qquad (7)$$

and provided $n = 2 j_1 + 1$ (otherwise j_1^{n+1} is lower). From (1) and (2) we now get that a necessary condition for the existence of (7) is:

$$P(j_2) - P(j_1) > E(j_2) - E(j_1) > 0. \qquad (8)$$

It will be recalled that in Mayer's model[8] the pairing energy of nucleons in some states is assumed to bring these "paired" states so much lower that $[E^*(j_2) - E^*(j_1)] < 0$. This is easily seen to be an extreme case of our considerations.

For the sake of brevity we should like to call the above effect as that of "delayed closing" of sub-shells.

Pt[195], Hg[197], and Hg[199] are all odd-neutron nuclei which have their odd neutron in the $(82 - 126)$ shell. The shell model predicts for neutrons in this shell the following states:

$$h_{9/2}, f_{7/2}, p_{3/2}, p_{1/2}, f_{5/2}, i_{13/2}.$$

The energy of the states probably increases in this order. As the pairing energy is bigger for states of higher spin, we could expect a delayed closing of sub-shells only when the higher sub-shell has a higher spin too. Thus in the $(82 - 126)$ neutron shell, the $p_{1/2}$ could remain unfilled while the upper sub-shells $f_{5/2}$ and $i_{13/2}$ are being filled.

Table VII contains the occupation numbers of the different levels for an odd nucleus which has 117 neutrons (such as Pt[195]), as would be predicted by the shell model for the first few excited configura-

Table VII.

Config.	$h_{9/2}$	$f_{7/2}$	$p_{3/2}$	$p_{1/2}$	$f_{5/2}$	$i_{13/2}$	Energy difference
G	10	8	4	1	6	6	0
A	10	8	4	0	6	7	$E(13/2) - E(1/2)$
B	10	8	4	2	5	6	$[E^*(1/2) - E^*(5/2)] - [E(1/2) - E(5/2)]$
C	10	8	3	2	6	6	$[E^*(1/2) - E^*(3/2)] - [E(1/2) - E(3/2)]$
D	10	8	4	2	6	5	$[E^*(1/2) - E^*(13/2)] - [E(1/2) - E(13/2)]$
E	10	8	4	2	3	8	$[E^*(1/2) - E(1/2)] - [E^*(5/2) - E(5/2)]$ $+ [E^*(13/2) - E^*(5/2)]$

Table VIII.

Element	Energy of γ-ray	Exp. α_K	Calculated α_K								Exp. K/L	Expected K/L								Ref.
			E1	E2	E3	E4	M1	M2	M3	M4		E1	E2	E3	E4	M1	M2	M3	M4	
Pt[195]	129	big		0,41	0,17	2,8	3,6	17,5	73	200	0,26			0,17				1,3	0,32	Present Work
Pt[195]	97	7,4 +8,2 −2,8		0,95	1,7	3,9	7,6	38	>160		5,8		<0,2			7,4	3,9			Present Work
Hg[197]	164	>4,6	0,17	0,47	0,97	1,8	3,4				0,45		0,42				1,7		0,52	10)
Hg[197]	133	0,5	0,12	0,32	0,67		2,3		27	86	0,42		0,41	0,17			1,3		0,32	10)
Hg[199]	157	0,33		0,16	0,32						0,67		0,40					1,65	0,30	Present Work
Hg[199]	208	0,98					0,94	8,0			5,65		1,0			7,8	6,0	2,4		Present Work
Hg[199]	368	>6,8				0,29				4,4	1,6		2,45	1,63	0,56		4,4		1,62	13)

tions, together with the energy difference between the lowest state of each configuration and the ground state G.

With the assumption of the single particle model the ground states of the configurations G, A, B, C, D, E are respectively: $p_{1/2}$, $i_{13/2}$, $f_{5/2}$, $p_{3/2}$, $i_{13/2}$, and $f_{5/2}$, and thus these should be the first few excited states in nuclei having 117 neutrons. It is easily seen that the same excited states should also occur in nuclei having any
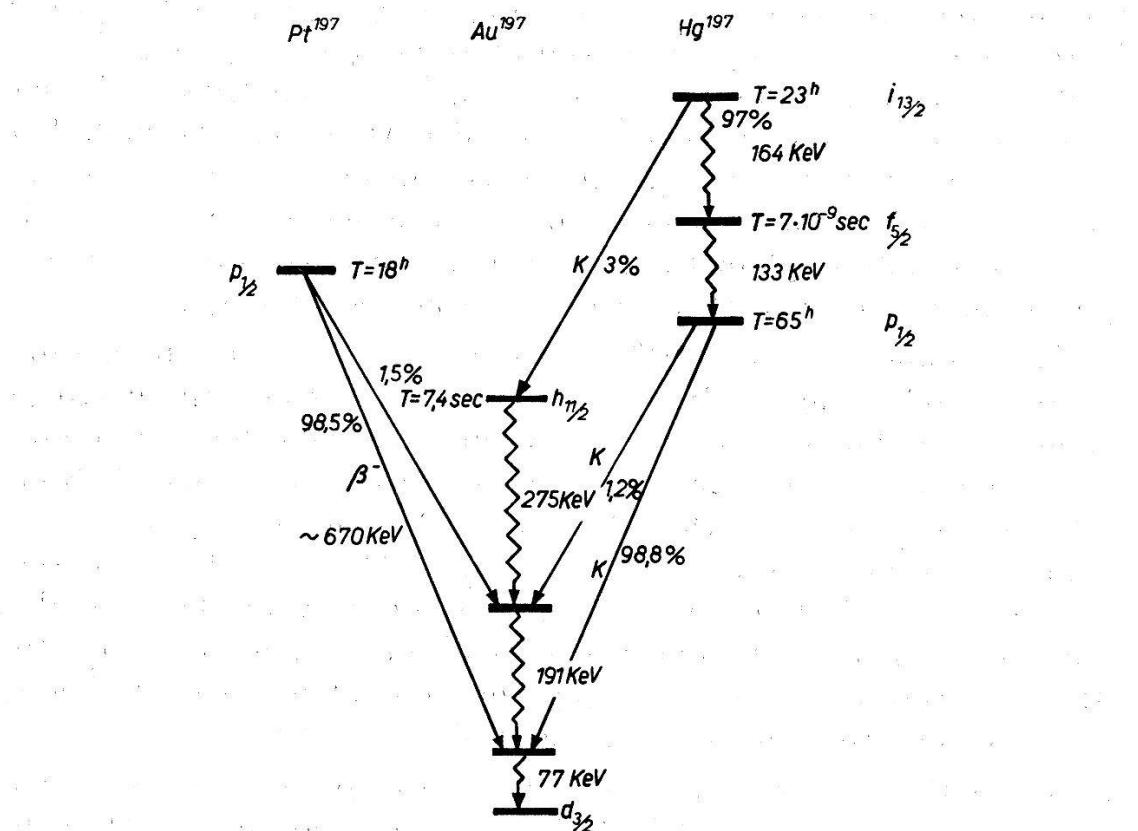

Fig. 9.
Decay scheme of Hg[197].

number of odd neutrons between 111 and 125, except the states A and D which do not appear at $N = 125$ and $N = 111$ respectively. States like E have little chances to be excited in usual cases since a transition to them usually involves a double nucleon transition and this is forbidden in a strict single particle model. Usually they are quite high too.

§ 2. Comparison with experiment.

Table VIII gives the experimental conversion coefficients and K/L ratios of some transitions in Pt and Hg, together with the calculated[18] values of α_K and the expected K/L ratios[19] for different multipole orders. For energies lower than 150 keV the values of α_K

were obtained by extrapolation. The expected K/L ratios were obtained by interpolation from the experimental graphs of K/L vs. Z^2/E; they are intended to give a rough estimate rather than an accurate value of the K/L ratio.

Pt^{195}.

The spin of Pt^{195} in the ground state is measured to be 1/2, and the magnetic moment suggests it is a $p_{1/2}$ state. The α_K of the 97 keV γ-ray could not be measured accurately because of its high value, but even with the relatively big error one sees from Table VIII that it could fit either with an E 4 or an M 1. However, the high K/L ratio of the 97 keV γ-ray and its short half-life ($< 10^{-6}$ sec as can be ascertained from our coincidence measurements) favour the M1 assignment rather than the E 4. Taking into account the spin of the ground state this shows that the 97 keV level is $p_{3/2}$.

The ground state of Au^{195} is probably $d_{3/2}$ (as are the ground states of Ir^{193} and Au^{197}, where both the spins and the magnetic moments are known). As the two K-captures from this state do not differ much in energy (29 keV) and are of the same order of intensity, we conclude that the 126 keV level could be $p_{1/2}$, $p_{3/2}$ or $f_{5/2}$ (opposite parity to that of $d_{3/2}$ and with $\Delta I = 0$ or 1). If it were $p_{1/2}$ or $p_{3/2}$ the 29 keV γ-ray and the 126 keV would both be M 1. This would not fit the experimental results which show that the 126 keV transition is less probable than the 29 keV one. We therefore conclude that the level at 126 keV is $f_{5/2}$.

As for the isomeric transition, its high conversion suggests it is a magnetic multipole, and its K/L ratio fixes it as an M 4. Thus the level at 255 keV is $i_{13/2}$.

Hg^{197}.

The spin of the ground state is probably 1/2 and the state is a $p_{1/2}$ (the same as in Hg^{199}). The 133 keV transition fits very well with an E 2 (Table VIII) and fixes the intermediate state as $f_{5/2}$. The half-life of the intermediate state also fits with the assignment of this multipole order for the 133 keV γ-ray[10]. The isomeric transition fits nicely the predicted values for α_K and K/L ratio of an M 4 transition. Thus the highest level is $i_{13/2}$.

A further evidence for the assignment of the spin 5/2 to the intermediate state is the $(e^- — e^-)$-angular correlation[20], which was shown to contain a $\cos^4 \vartheta$ term, thus proving that the intermediate state has a spin of at least 5/2 units.

Hg^{199}.

The measured spin and magnetic moments of the ground state suggest it is a $p_{1/2}$ one. The 157 keV γ-ray fits best with an E 2 transition, thus fixing the 157 keV level as $f_{5/2}$. The branching of the level at 208 keV suggests that the 51 keV γ-ray and the 208 keV one are of the same multipole order. The conversion of the 208 keV γ-ray fixes it as an M 1 transition, thus suggesting that the level at 208 keV is $p_{3/2}$. The isomeric transition is again M 4, and the isomeric state — $i_{13/2}$. The absence of angular correlation between the β-spectrum from Au^{199} and any of the following γ-rays supports this spin assignment for the different levels in Hg^{199}.

§ 3. Conclusion.

It is seen that all the single particle states predicted by the shell model appear in these nuclei and no other levels are found. (The $p_{3/2}$ is not found experimentally in Hg^{197}; this could be wholly attributed to the mode of exciting the levels in this nucleus. If the $p_{3/2}$ state is above the $f_{5/2}$ or below and very near to it one cannot expect its being excited via a transition from the isomeric state or from the $f_{5/2}$ state. This is clearly seen in Hg^{199}.)

The relative positions of the different levels change continuously by adding two protons or two neutrons: the energy of the isomeric transition increases with a resulting decrease in the half-life. The energy of the E 2 transition which follows the isomeric state increases too with A, though less rapidly. The $p_{3/2}$ level moves upwards in relation to the $f_{5/2}$ level as one adds pairs of protons or neutrons.

It is perhaps instructive to compare this behavior of the energy levels with the behavior of the corresponding levels at the end of the (50—82) shell as exhibited by different isotopes of Te, Xe, and Ba. There, too, the isomeric transition $(h_{11/2} - d_{3/2})$ increases in energy as one adds pairs of equivalent nucleons, and in the same time the $s_{1/2}$ level moves upwards in relation to the $d_{3/2}$ one, and indeed crosses it, very much the same as the $p_{3/2}$ crosses the $f_{5/2}$ level in the (82—126) shell.

It is hoped that further study of other odd A isotopes of Hg, Pt, Os, etc. will show whether the excellent accord of the hitherto measured isotopes with the single particle model is accidental or real.

References.

[1]) W. ELSASSER, J. de phys. et rad. **5,** 625 (1934).

[2]) M. G. MAYER, Phys. Rev. **74,** 235 (1948).

[3]) H. E. SUESS, Phys. Rev. **81,** 1071 (1951).

[4]) HAXEL, JENSEN, and SUESS, Phys. Rev. **75,** 1766 (1949).

[5]) E. FEENBERG and K. C. HAMMACK, Phys. Rev. **75,** 1877 (1949).

[6]) L. W. NORDHEIM, Phys. Rev. **75,** 1894 (1949).

[7]) M. G. MAYER, Phys. Rev. **75,** 1969 (1949).

[8]) M. G. MAYER, Phys. Rev. **78,** 16 (1950).

[9]) A. DE-SHALIT, to be published.

[10]) O. HUBER, F. HUMBEL, H. SCHNEIDER, A. DE-SHALIT, and W. ZÜNTI, Helv. Phys. Acta **24,** 127 (1951).

[11]) O. HUBER, F. HUMBEL, H. SCHNEIDER and A. DE-SHALIT, Helv. Phys. Acta **25,** 3 (1952).

[12]) H. SCHNEIDER, O. HUBER, and A. DE-SHALIT, Helv.Phys. Acta **25,** 259 (1952).

[13]) K. WAY, L. FANO, M. SCOTT, and K. THEW, Nuclear Data, Circular of the N.B.S. No. 499.

[14]) We are indebted to Mr. H. HUBER for performing this experiment.

[15]) R. D. HILL, Phys. Rev. **79,** 413 (1950); P. M. SHERK and R. D. HILL, Phys. Rev. **83,** 1097 (1951).

[16]) O HUBER, F. HUMBEL, H. SCHNEIDER, and W. ZÜNTI, Helv. Phys. Acta **23,** 855 (1950).

[17]) H. S. W. MASSEY and E. H. S. BURHOP, Proc. Roy. Soc., A, **153,** 661 (1936).

[18]) ROSE, SPINARD, GOERTZEL, HAAR, and STRONG (privately circulated report).

[19]) M. GOLDHABER and A. W. SUNYAR, Phys. Rev.

[20]) H. FRAUENFELDER, M. WALTER, and W. ZÜNTI, Phys. Rev. **77,** 557 (1950).